Journal of Catalysis **192,** 197–203 (2000)
doi:10.1006/jcat.2000.2832, available online at http://www.idealibrary.com on IDEAL®

Kinetic Isotopic Effects in Oxidative Dehydrogenation of Propane on Vanadium Oxide Catalysts

Kaidong Chen, Enrique Iglesia,[1] and Alexis T. Bell[1]

Chemical and Materials Sciences Divisions, Lawrence Berkeley National Laboratory, and Department of Chemical Engineering, University of California, Berkeley, California 94720-1462

Received October 25, 1999; accepted January 28, 2000

Kinetic isotopic effects (KIEs) for oxidative dehydrogenation of propane were measured on 10 wt% V_2O_5/ZrO_2. Normal KIEs were obtained using $CH_3CH_2CH_3$ and $CD_3CD_2CD_3$ as reactants for primary dehydrogenation (2.8) and combustion (1.9) of propane and for secondary combustion of propene (2.6), suggesting that in all cases C–H bond dissociation is a kinetically relevant step. $CH_3CH_2CH_3$ and $CH_3CD_2CH_3$ reactants led to normal KIEs for dehydrogenation (2.7) and combustion (1.8) of propane, but to a very small KIE (1.1) for propene combustion. These results show that the methylene C–H bond is activated in the rate-determining steps for propane dehydrogenation and combustion reactions. The rate-determining step in secondary propene combustion involves the allylic C–H bond. In each reaction, the weakest C–H bond in the reactant is cleaved in the initial C–H bond activation step. The measured propane oxidative dehydrogenation KIEs are in agreement with theoretical estimates using a sequence of elementary steps, reaction rate expression, and transition state theory. The much smaller KIE for propane oxidative dehydrogenation (2.8) than the maximum KIE (6) expected for propane thermal dehydrogenation indicates the participation of lattice oxygen. The different KIE values for propane primary dehydrogenation and combustion suggest that these two reactions involve different lattice oxygen sites.

Key Words: **propane; oxidative dehydrogenation; vanadium oxide.**

INTRODUCTION

Oxidative dehydrogenation (ODH) of alkanes is thermodynamically favored over a wide temperature range and offers the potential for the synthesis of alkenes with significant savings in energy and feedstock costs (1–5). Propane ODH occurs via the parallel and sequential oxidation steps shown in Scheme 1 (1). Propene is a primary product and carbon oxides (CO_x) form directly from propane and by subsequent oxidation of propene. The most active and selective catalysts for propane ODH are based on supported vanadia (3). On VO_x-based catalysts, ODH rate expressions and reaction mechanisms have been reported (6–8). Reaction rates are proportional to propane pressure and generally independent of the pressure of O_2. The reaction involves Mars–van Krevelen redox pathways with lattice oxygen involved in rate-determining C–H bond activation steps (2, 8). Methylene C–H bonds in propane are weaker than those of the methyl groups; as a result, propane activation has been proposed to occur by the initial cleavage of these weaker C–H bonds to form isopropoxide species (2), without direct experimental evidence. Kinetic isotope effects for undeuterated, perdeuterated, and selectively deuterated propane molecules can be used to discern the rate-determining nature of C–H activation steps and the position of the activated C–H bond. The replacement of H with D at the position of C–H activation decreases the rate of reactions limited by C–H bond cleavage, leading to normal kinetic isotope effects (KIEs; $k_H/k_D > 1$).

Polyvanadate structures on ZrO_2 appear to provide an optimum compromise between the reducibility and the accessibility of VO_x domains and they lead to more active catalysts than VO_x dispersed on other supports (9, 10). The reaction rate constant ratio (k_1/k_2) for primary dehydrogenation (k_1) and primary combustion (k_2) increases with increasing VO_x surface density (9), suggesting that the two reactions require different sites. Kinetic and isotopic tracer studies showed that the activation of C–H bonds is involved in rate-determining steps (8). Here, we provide supporting evidence for the proposed mechanism by examining ODH reaction rates and selectivities for $CH_3CH_2CH_3$, $CH_3CD_2CH_3$, and $CD_3CD_2CD_3$ reactants.

EXPERIMENTAL

V_2O_5/ZrO_2 (10 wt%) was prepared by incipient wetness impregnation methods and treated in air at 773 K, as described in Ref. (9). X-ray diffraction, X-ray absorption, Raman, and UV–visible methods showed that this sample consists of two-dimensional polyvanadate structures on a predominately tetragonal ZrO_2 surface (9, 10).

---

[1] Authors to whom correspondence should be addressed (bell@cchem.berkeley.edu; iglesia@cchem.berkeley.edu).

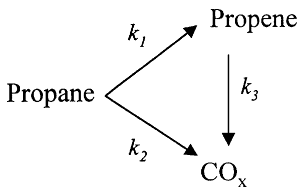

SCHEME 1. Reaction network for the oxidative dehydrogenation of propane.

Reaction rates were measured using a gradientless batch reactor consisting of a shallow packed bed within a gas recirculation loop (11). Reactants and products were recirculated at $3.3\,\mathrm{cm^3\,s^{-1}}$ using a graphite gear micropump in order to achieve low propane conversions (<1%) per pass. The chemical composition of the recirculating stream was determined by gas chromatography (Hewlett-Packard 6890), and the isotopic content by mass spectrometry/gas chromatography (Hewlett-Packard 5972). Mass spectra were used to calculate the deuterium content and the isotopomer contribution in each reactant and product molecule using deconvolution methods reported previously (12). Reaction rates were extrapolated to zero reaction time in order to obtain initial reaction rates and rate constants. Undeuterated propane (Matheson, instrument purity >99.5%), perdeuterated propane (Isotec, chemical purity >99.0%, isotopic purity >99.0%), propane-2,2-d_2 (Isotec, chemical purity >99.0%, isotopic purity >99.0%), oxygen (research grade, >99.999%), and propene (Matheson, chemical purity >99.0%) were used as reactants without further purification. Perdeuterated water (D_2O; Isotec, chemical purity >99.0%, isotopic purity >99.0%) was purified by several freeze–thaw evacuation cycles before use. Helium (research grade, >99.999%) was used as an inert diluent.

RESULTS AND DISCUSSION

As reported earlier (9), propane ODH on VO_x/ZrO_2 occurs via parallel and sequential steps as shown in Scheme 1. At relatively low conversions and low H_2O concentrations, the rate of each reaction is well described by

$$r_1 = k_1[C_3H_8] \quad [1]$$

$$r_2 = k_2[C_3H_8] \quad [2]$$

$$r_3 = k_3[C_3H_6], \quad [3]$$

where k_i is the apparent first-order rate coefficient for reaction i. The propene selectivity at relatively low conversions in a batch reactor is given by (10)

$$S = S^0[1 - (k_3C_V/2)t], \quad [4]$$

where C_V is the concentration of V atoms per unit reactor volume, t is the reaction time, and S^0 [$=k_1/(k_1+k_2)$] is the initial propene selectivity (at zero conversion). The value of k_1 is determined from the initial rate of propene conversion (as $t \rightarrow 0$) and the value of k_2 from the initial propene selectivity (S^0). The value of k_3 is then calculated from the dependence of propene selectivity on time, as predicted by Eq. [4]. Figure 1 shows an example of the propene formation rate and selectivity versus reaction time.

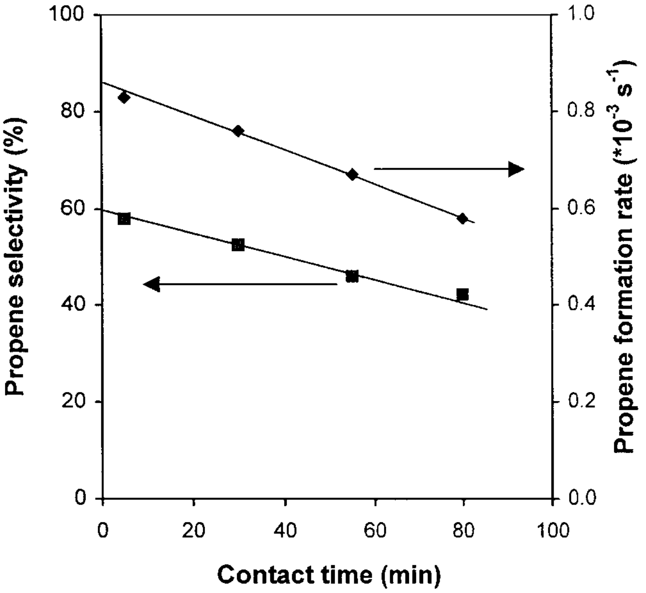

FIG. 1. Propene selectivity and formation rate in the reaction of propane/oxygen mixtures on 10 wt% VO_x/ZrO_2 in a batch reactor (593 K, 14.2 kPa propane, 1.7 kPa O_2, balance He).

Reaction rate constants ($k_{i,\mathrm{C-H}}$ and $k_{i,\mathrm{C-D}}$) for ODH of undeuterated propane, perdeuterated propane, and propane-2, 2-d_2 were obtained from the rate of initial propene formation measured for reaction mixtures containing $CH_3CH_2CH_3/O_2$, $CD_3CD_2CD_3/O_2$, or $CH_3CD_2CH_3/O_2$. Kinetic isotope effects (defined as the ratio of $k_{i,\mathrm{C-H}}/k_{i,\mathrm{C-D}}$) for reactions 1, 2, and 3 are shown in Table 1. Results obtained with $CH_3CH_2CH_3/O_2$ and $CD_3CD_2CD_3/O_2$ gave kinetic isotope effects greater than unity for all three reaction steps, confirming that C–H bond dissociation is a kinetically relevant step (8). The KIE values for propane ODH (2.8) and propane combustion (1.9) are different, suggesting that

TABLE 1

Kinetic Isotopic Effects over 10 wt% VO_x/ZrO_2 Catalyst (593 K, 14.2 kPa Propane, 1.7 kPa O_2, Balance He)

Isotope	$CH_3CH_2CH_3/$ $CD_3CD_2CD_3$	$CH_3CH_2CH_3/$ $CH_3CD_2CH_3$	$CH_3CD_2CH_3/$ $CD_3CD_2CD_3$
Primary dehydrogenation, $k_{1,\mathrm{C-H}}/k_{1,\mathrm{C-D}}$	2.8	2.7	1.0
Secondary combustion, $k_{3,\mathrm{C-H}}/k_{3,\mathrm{C-D}}$	2.6	1.1	2.5
Primary combustion, $k_{2,\mathrm{C-H}}/k_{2,\mathrm{C-D}}$	1.9	1.8	1.1

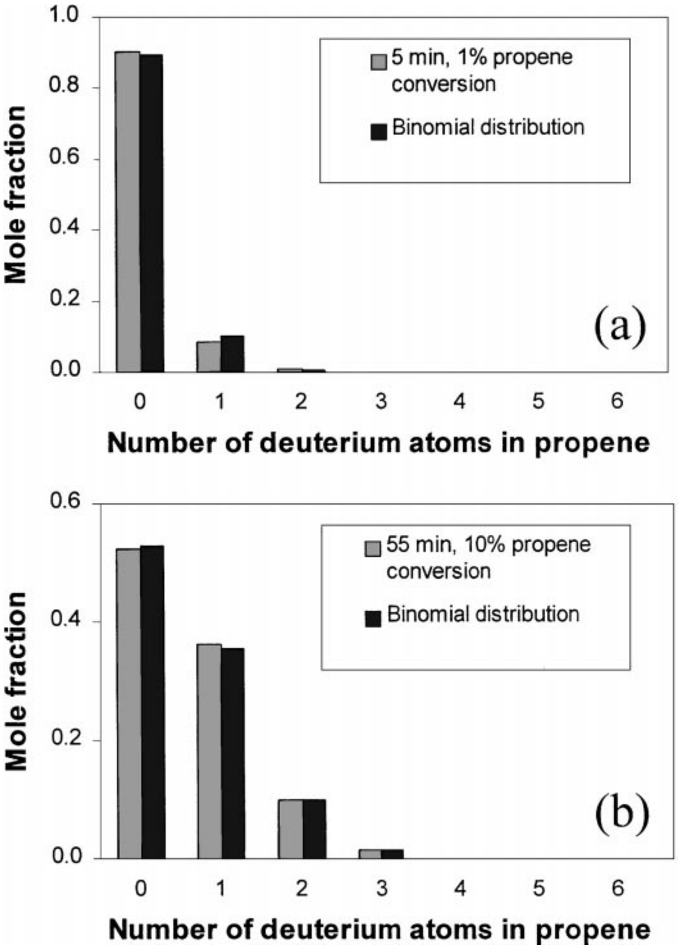

FIG. 2. Deuterium distribution in unreacted propene in $C_3H_6/D_2O/O_2$ mixtures on 10 wt% VO_x/ZrO_2 in a batch reactor. (a) 1% propene conversion, H/D molar ratio in propene is 54, and (b) 10% propene conversion, H/D molar ratio in propene is 9 (593 K, 2.1 kPa propene, 1.7 kPa O_2, 0.8 kPa D_2O, balance He).

the formation of propene and CO_x from propane involves different active sites (see below). These results are consistent with those reported in the literatures (9, 10).

The activation of both propane and propene involves the cleavage of C–H bonds in kinetically relevant steps. There are two kinds of C–H bonds in molecular propane; the methyl C–H bonds have a dissociation enthalpy of 420 kJ/mol and the methylene C–H bonds have a dissociation enthalpy of 401 kJ/mol (13). KIE measurements using $CH_3CH_2CH_3$ and $CD_3CD_2CD_3$ cannot determine which C–H bond is involved in the initial activation step. On the other hand, $CH_3CD_2CH_3$ is expected to react more slowly than $CH_3CH_2CH_3$ if methylene C–H bonds are involved in the initial activation step. Similar rates for $CH_3CD_2CH_3$ and $CD_3CD_2CD_3$ would indicate that only the methylene C–H bonds are involved in the rate-determining step and that the isotopic content of the rest of the propane molecule does not influence reaction rates. The data in Table 1 show that $CH_3CD_2CH_3$ exhibits a normal KIE for both propane dehydrogenation (2.7) and combustion (1.8). These values are almost identical to those obtained using $CD_3CD_2CD_3$ (2.8 and 1.9, respectively), confirming the hypothesis that methylene C–H bonds are the only ones involved in the rate-determining steps for both propane dehydrogenation and combustion. Similar isotopic studies for butane oxidation to maleic anhydride have led to the similar conclusion that methylene C–H bonds are activated preferentially during the initial phase of the process (14).

Kinetic isotopic effects for propene combustion were determined from the effect of contact time on propene selectivity (Table 1); however, it is not possible to conclude which particular bond cleaves in the rate-determining step for this reaction just by simple inspection of the KIE for the reaction of $CH_3CD_2CH_3/O_2$. Propene exchanges rapidly with available adsorbed H and D species during ODH, leading to statistical distribution of D atoms, as shown in studies of C_3H_8/D_2O over VO_x/ZrO_2 (8). Therefore, propene formed from $CH_3CD_2CH_3/O_2$ contains CH_3CDCH_2, as well as all the other isotopomers of C_3H_5D and $C_3H_4D_2$, etc. Consequently, the observed KIE reflects an average value for all propene isotopomers.

Previous results show that water can also exchange with H and D present on the catalyst surface during ODH (8). Figures 2 and 3 show the results for the reaction of $C_3H_6/D_2O/O_2$. At all propene conversion levels (1–20%), the deuterium distribution in the unreacted propene obeys a binomial distribution rule (Fig. 2). This confirms that H/D exchange of propene with the catalyst surface is very fast and quasi-equilibrated, so the H/D ratio in propene is equal to the H/D ratio in the surface H/D pool. However, the H/D ratio in the unreacted propene is very large initially and decreases with reaction time, reaching steady state

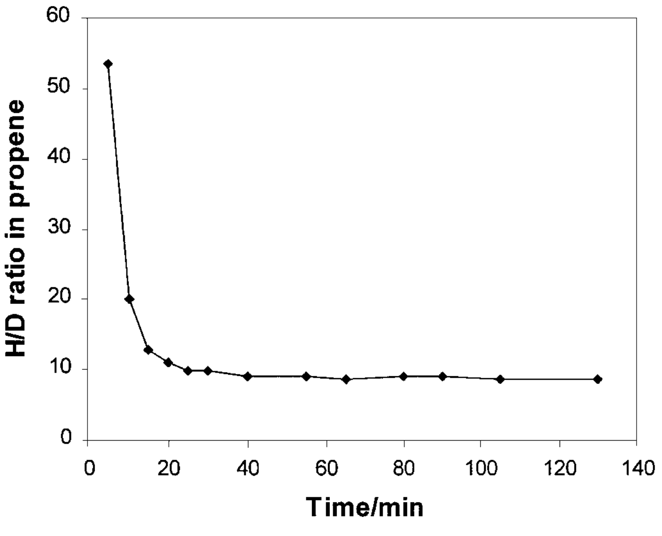

FIG. 3. H/D molar ratio in unreacted propene in a $C_3H_6/D_2O/O_2$ mixture on 10 wt% VO_x/ZrO_2 in a batch reactor (593 K, 2.1 kPa propene, 1.7 kPa O_2, 0.8 kPa D_2O, balance He).

after ~20 min (Fig. 3). This suggest that during the reaction, gas-phase water exchanges H and D with the surface H/D pool (because all D in the surface pool comes from D_2O), but that this step is much slower than the rate at which propene exchanges with the surface H/D pool. With increasing contact time, the concentration of D in the surface H/D pool increases because of the exchange of H in the pool with D_2O. This, in turn, causes the H/D ratio in the surface pool, and in propene, to decrease. However, the deuterium concentration in water decreases during the course of the reaction because D_2O is diluted by the formation of H_2O. The deuterium concentrations in the catalyst surface H/D pool, propene, and gas-phase water finally equilibrate.

The discussion of how $C_3H_6/D_2O/O_2$ reacts demonstrates that the exchange of the catalyst surface H/D pool with water is much slower than with propene. As a consequence, the initial D/H ratio in the propene formed from a $CH_3CD_2CH_3/O_2$ mixture should be close to 1 : 5. Propene has three kinds of C–H bonds. The weakest C–H bonds are the allylic ones which have a dissociation enthalpy of 361 kJ/mol (13). Previous studies of propene oxidation to acrolein (15–17) have shown that the weakest allylic C–H bonds are activated. Assuming that the allylic C–H bonds of propene are dissociated preferentially during propene combustion, the KIE associated with the combustion of propene derived from $CH_3CD_2CH_3$ was calculated. A base case KIE value of 2.6 for the combustion of C_3H_6 versus C_3D_6 was taken for these calculations. The calculated KIE for propene combustion (assuming an initial D/H ratio of 5) for $CH_3CH_2CH_3$ versus $CH_3CD_2CH_3$ is 1.14, which is very close to the value found experimentally, 1.1. Similarly, the calculated KIE for propene combustion for $CH_3CD_2CH_3$ versus $CD_3CD_2CD_3$ is 2.45, whereas that seen experimentally is 2.5. These results provide indirect evidence that the weakest C–H bond in propene, i.e., the allylic C–H bond, is dissociated preferably during propene oxidation. Also shown in Table 2 are the KIE values calculated under the assumption the initial D/H ratio in propene for $CH_3CD_2CH_3/O_2$ reaction is 2 : 6. These values do not agree with the experimental ones as well, confirming that the exchange of the catalyst surface H/D pool with water is much slower than that with propene.

TABLE 2

Calculated Kinetic Isotopic Effects for Propene Combustion Reaction over 10 wt% VO_x/ZrO_2 Catalyst at 593 K

	KIE for different isotopes	
D/H ratio[a]	$CH_3CH_2CH_3$/ $CH_3CD_2CH_3$	$CH_3CD_2CH_3$/ $CD_3CD_2CD_3$
1 : 5	1.14	2.45
2 : 6	1.22	2.37

[a] Initial D/H ratio in propene during the ODH of $CH_3CD_2CH_3$.

The measured KIE values are reasonable and reflect the participation of lattice oxygen species during propane ODH reaction. ODH kinetics over VO_x/ZrO_2 catalysts have been studied in detail and the kinetic rate expression has also been obtained (8). Propane ODH is envisioned to occur via the following sequence:

1. Weak associative adsorption of propane on lattice oxygen (O^*),

$$C_3H_8 + O^* \rightleftarrows C_3H_8O^*. \qquad [I]$$

2. C–H cleavage via H-abstraction from propane using a neighboring lattice oxygen,

$$C_3H_8O^* + O^* \rightarrow C_3H_7O^* + OH^*. \qquad [II]$$

3. Desorption of propene by hydride elimination from adsorbed alkoxide species,

$$C_3H_7O^* \rightarrow C_3H_6 + OH^*. \qquad [III]$$

4. Recombination of OH groups to form water and a reduced V center (*),

$$OH^* + OH^* \rightleftarrows H_2O + O^* + {}^*. \qquad [IV]$$

5. Reoxidation of reduced V centers via dissociative chemisorption of O_2,

$$O_2 + {}^* + {}^* \rightarrow O^* + O^*. \qquad [V]$$

In this scheme, O^* is a lattice oxygen atom in the VO_x overlayer (e.g., V=O, V–O–V, or V–O–Zr), OH^* is a hydroxyl group in V–O–H, $C_3H_7O^*$ represents an adsorbed propoxide bonded to V (V–O–C_3H_7), and * represents a surface vacancy associated with either one V^{3+} or two V^{4+} cations in the VO_x lattice. These elementary steps, together with pseudo-steady-state assumptions for all adsorbed intermediates and quasi-equilibrium assumptions for steps (II) and (IV), lead to a rate expression of the form

$$r = k_{II}K_I[C_3H_8]/\{1 + (K_{IV}[H_2O])^{0.5} \times (k_{II}K_I[C_3H_8]/2k_V[O_2])^{0.25}\}^2, \qquad [5]$$

where k_i is the rate coefficient and K_i is the equilibrium constant for step i. At low H_2O concentrations, the rate of propane ODH given by Eq. [5] becomes

$$r = k_{II}K_I[C_3H_8] = k_1[C_3H_8]. \qquad [6]$$

The apparent rate coefficient k_1 is, therefore, equal to $k_{II}K_I$. The theoretical KIE of propane ODH can be calculated on the basis of elementary steps I and II, Eq. [6], and transition state theory (18, 19). As shown in the Appendix, if lattice oxygen does not participate in C–H bond activation of propane, i.e., the transition state involves only the homogeneous dissociation of the C–H bond and no O–H and

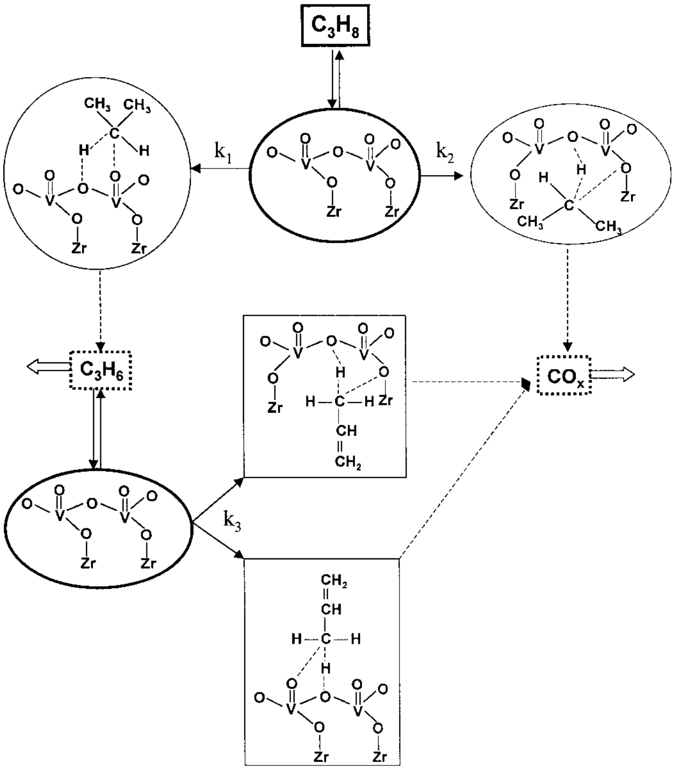

FIG. 4. Proposed reaction pathways for propane reactions on VO_x-based catalysts.

C–O bonds are formed, the theoretical KIE at 593 K will be ca. 6. This value is much larger than what we observe (2.8). However, when the activation of the C–H bond includes the participation of lattice oxygen, i.e., C–H bond cleavage is accompanied by formation of C–O and O–H bonds, the KIE becomes smaller. The experimental KIE value of 2.8 suggests that the transition state for ODH involves the formation of C–O and O–H bonds as well as the weakening of a C–H bond (i.e., participation of lattice oxygen in C–H bond activation). This conclusion is consistent with that obtained by reacting C_3H_8/O_2^{18} over VO_x^{16}/ZrO_2 (8).

The theoretical calculations presented in the Appendix cannot prove why the KIE for propane primary dehydrogenation is larger than that for propane combustion. However, they do provide a qualitative explanation for why the KIEs for these two reactions are different. As noted earlier, lattice oxygen participates in C–H bond activation. Previous results have shown that the reaction rate constant ratio (k_1/k_2) for primary dehydrogenation (k_1) and primary combustion (k_2) increases with the increase of VO_x surface density (9), suggesting that the two reactions require different sites; e.g., V=O or V–O–V bonds are involved in primary dehydrogenation, while the V–O–Zr bond is involved in primary combustion reactions. If the lattice oxygen species participating in the propane primary dehydrogenation and combustion reactions are different, it is expected that the strengths of the O–H bonds formed in the two transition states are different, and, hence on the basis of Eq. [A22], the KIEs for these two reactions will be different.

The proposed pathways for the activation of propane and propene deduced from the isotopic labeling experiments reported here and those reported earlier (8, 9) are summarized in Fig. 4. Propane can either interact with V=O or V–O–V bonds at selective oxidation sites forming propene (k_1), or interact with V–O–Zr bonds at combustion sites forming CO_x (k_2). In both cases, the secondary C–H bond in propane dissociated preferentially. The primary dehydrogenation product propene can either desorb or readsorb on dehydrogenation and combustion sites where it is then converted to CO_x (k_3). The weakest C–H bond in propene, i.e., the allylic C–H bond, is preferably dissociated during combustion reaction.

CONCLUSIONS

Measurements of kinetic isotopic effects using undeuterated ($CH_3CH_2CH_3$), perdeuterated ($CD_3CD_2CD_3$), and selectively deuterated propane ($CH_3CD_2CH_3$) molecules can be used to identify the kinetic significance of C–H bond activation steps and the position of the C–H involved in oxidative dehydrogenation. Normal KIEs for propane primary dehydrogenation (2.8) and combustion (1.9) and for propene secondary combustion reactions (2.6) were obtained when $CH_3CH_2CH_3$ and $CD_3CD_2CD_3$ were used as reactants, suggesting that in all cases C–H bond dissociation is a kinetically relevant step. Comparison of $CH_3CH_2CH_3$ and $CH_3CD_2CH_3$ as reactants led to normal KIEs for dehydrogenation (2.7) and combustion (1.8) of propane, confirming that the methylene C–H bond is activated in the rate-determining steps for propane dehydrogenation and combustion. It is expected that the rate-determining step in secondary propene combustion involves activation of an allylic C–H bond. The measured propane oxidative dehydrogenation KIE values are consistent with those theoretically predicted. The smaller KIE for propane oxidative dehydrogenation (2.8) than the maximum KIE (6) expected for propane thermal dehydrogenation indicates the participation of lattice oxygen. The difference in the KIE values for propane primary dehydrogenation and combustion reactions reflects that these two reactions involve different lattice oxygen species.

APPENDIX: THEORETICAL TREATMENT OF KINETIC ISOTOPE EFFECT

The appropriate equations for translational, rotational, electronic, and vibrational partition functions at 600 K are

$$Q_{\text{trans}} = \frac{(2\pi m k_b T)^{3/2} V}{h^3} \propto (mT)^{3/2} \qquad [A1]$$

$$Q_{\mathrm{rot}} = \frac{8\pi^2}{\sigma h^3}(2\pi k_{\mathrm{b}} T)^{3/2}(I_x I_y I_z)^{1/2} \propto T^{3/2}(I_x I_y I_z)^{1/2} \qquad \text{[A2]}$$

$$Q_{\mathrm{elec}} = g_0 + g_1\,\mathrm{e}^{-\varepsilon_1/k_{\mathrm{b}}T} + g_2\,\mathrm{e}^{-\varepsilon_2/k_{\mathrm{b}}T} + \cdots \approx g_0 = \mathrm{e}^{-\varepsilon_0/RT} \qquad \text{[A3]}$$

$$Q_{\mathrm{vib}} = \sum_{\nu=0}^{\infty} \mathrm{e}^{-\nu\theta_\nu/T} \approx \frac{1}{1-\mathrm{e}^{-\theta_\nu/T}}, \quad \text{where} \quad \theta_\nu = \frac{h}{2\pi k_{\mathrm{b}}}\sqrt{\frac{k}{\mu}}. \qquad \text{[A4]}$$

The constants and variables in the equations above are defined as follows: h = Planck's constant; I_x, I_y, I_z = moments of inertia; k = force constant; k_{b} = Boltzmann's constant; m = mass of molecules or atoms; T = temperature (K); V = volume; $\mu = m_1 m_2/(m_1 + m_2)$ = reduced mass; ε_0 = zero-point energy; σ = symmetry number; and θ_ν = characteristic temperature for vibration (K).

For gas-phase molecules all four partition functions are important. However, the translational partition function is unity for immobile adsorbed species.

For oxidation of propane reaction, the rate of propane ODH is proportional to

$$\text{rate} \propto K_{\mathrm{I}} k_{\mathrm{II}}. \qquad \text{[A5]}$$

Therefore, the kinetic isotope effect (KIE), which is defined as the ratio of ODH reaction rates for C_3H_8/O_2 to C_3D_8/O_2 mixtures, equals

$$\mathrm{KIE} = \left(\frac{K_{\mathrm{I},C_3H_8}}{K_{\mathrm{I},C_3D_8}}\right)\left(\frac{k_{\mathrm{II},C_3H_8}}{k_{\mathrm{II},C_3D_8}}\right). \qquad \text{[A6]}$$

Each ratio in parentheses in Eq. [A6] is examined separately as follows.

$$(1),\ \frac{k_{\mathrm{II},C_3H_8}}{k_{\mathrm{II},C_3D_8}} = \frac{\left(\frac{Q^{\Xi}_{C_3H_7O^*OH^*}}{Q_{C_3H_8O^*}\,Q_{O^*}}\right)}{\left(\frac{Q^{\Xi}_{C_3D_7O^*OD^*}}{Q_{C_3D_8O^*}\,Q_{O^*}}\right)} = \left(\frac{Q^{\Xi}_{C_3H_7O^*OH^*}}{Q^{\Xi}_{C_3D_7O^*OD^*}}\right)\left(\frac{Q_{C_3D_8O^*}}{Q_{C_3H_8O^*}}\right) \qquad \text{[A7]}$$

$$(2),\ \frac{K_{\mathrm{I},C_3H_8}}{K_{\mathrm{I},C_3D_8}} = \frac{\left(\frac{Q_{C_3H_8O^*}}{Q_{C_3H_8}\,Q_{O^*}}\right)}{\left(\frac{Q_{C_3D_8O^*}}{Q_{C_3D_8}\,Q_{O^*}}\right)} = \left(\frac{Q_{C_3H_8O^*}}{Q_{C_3D_8O^*}}\right)\left(\frac{Q_{C_3D_8}}{Q_{C_3H_8}}\right). \qquad \text{[A8]}$$

Combining Eqs. [A6] through [A8] results in

$$(3),\ \mathrm{KIE} = \left(\frac{Q^{\Xi}_{C_3H_7O^*OH^*}}{Q^{\Xi}_{C_3D_7O^*OD^*}}\right)\left(\frac{Q_{C_3D_8}}{Q_{C_3H_8}}\right). \qquad \text{[A9]}$$

Each ratio of partition functions is evaluated as follows.

(1) Translational partition function contribution:

$$\left(\frac{Q_{C_3D_8}}{Q_{C_3H_8}}\right)_{\mathrm{trans}} = \left(\frac{m_{C_3D_8}}{m_{C_3H_8}}\right)^{3/2} = \left(\frac{52}{44}\right)^{3/2} = 1.285. \qquad \text{[A10]}$$

The $C_3H_7O^*OH^*$ and $C_3D_7O^*OD^*$ adsorbed species have zero translational degrees of freedom, and the reduced masses of $C_3H_7O^*OH^*$ and $C_3D_7O^*OD^*$ adsorbed species are approximately the same. Therefore,

$$\left(\frac{Q^{\Xi}_{C_3H_7O^*OH^*}}{Q^{\Xi}_{C_3D_7O^*OD^*}}\right)_{\mathrm{trans}} \approx 1. \qquad \text{[A11]}$$

(2) Rotational partition function contribution:

$$\left(\frac{Q_{C_3D_8}}{Q_{C_3H_8}}\right)_{\mathrm{rot}} = \left(\frac{(I_x I_y I_z)_{C_3D_8}}{(I_x I_y I_z)_{C_3H_8}}\right)^{1/2} = \left(\frac{28.1 \times 80.7 \times 90.3}{16.9 \times 59.8 \times 67.5}\right)^{1/2} = 1.733. \qquad \text{[A12]}$$

The $C_3H_7O^*OH^*$ and $C_3D_7O^*OD^*$ are adsorbed species, therefore,

$$\left(\frac{Q^{\Xi}_{C_3H_7O^*OH^*}}{Q^{\Xi}_{C_3D_7O^*OD^*}}\right)_{\mathrm{rot}} \approx 1. \qquad \text{[A13]}$$

(3) Vibrational partition function contribution: at low temperature, when $T < 1000$ K,

$$\left(\frac{Q_{C_3D_8}}{Q_{C_3H_8}}\right)_{\mathrm{vib}} \approx 1 \qquad \text{[A14]}$$

$$\left(\frac{Q^{\Xi}_{C_3H_7O^*OH^*}}{Q^{\Xi}_{C_3D_7O^*OD^*}}\right)_{\mathrm{vib}} \approx 1. \qquad \text{[A15]}$$

(4) Electronic partition function contribution:

$$\left(\frac{Q_{C_3D_8}}{Q_{C_3H_8}}\right)_{\mathrm{elec}} = \mathrm{e}^{\left(E_{C_3H_8} - E_{C_3D_8}\right)/RT} \qquad \text{[A16]}$$

$$\left(\frac{Q^{\Xi}_{C_3H_7O^*OH^*}}{Q^{\Xi}_{C_3D_7O^*OD^*}}\right)_{\mathrm{elec}} = \mathrm{e}^{\left(E^{\Xi}_{C_3D_7O^*OD^*} - E^{\Xi}_{C_3H_7O^*OH^*}\right)/RT}. \qquad \text{[A17]}$$

Combining Eqs. [A9] through [A17], the kinetic isotopic effect can be approximated as

$$\begin{aligned}\mathrm{KIE} &= 2.23\,\mathrm{e}^{\left[\left(E_{C_3H_8} - E^{\Xi}_{C_3H_7O^*OH^*}\right) - \left(E_{C_3D_8} - E^{\Xi}_{C_3D_7O^*OD^*}\right)\right]/RT} \\ &= 2.23\,\mathrm{e}^{(\Delta E_{\mathrm{H}} - \Delta E_{\mathrm{D}})/RT} = 2.23\,\mathrm{e}^{\Delta(\Delta E)/RT}. \qquad \text{[A18]}\end{aligned}$$

ΔE_{H} is the zero-point energy difference between C_3H_8 and the corresponding transition state species, while ΔE_{D} is the zero-point energy difference between C_3D_8 and the corresponding transition state species, and $\Delta(\Delta E)$ reflects the difference between ΔE_{H} and ΔE_{D}. The zero-point energy of the transition state species cannot be determined; however, as shown in Fig. A1, comparing propane and the corresponding transition state, the main difference in energy is the full C–H bond in propane changes to partially formed

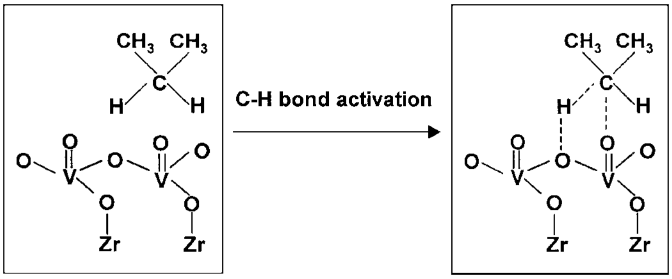

FIG. A1. Speculated transition state during C–H bond activation of propane ODH.

C–O, O–H, and C–H bonds in the transition state. So ΔE_{H} can be approximately expressed as

$$\begin{aligned}\Delta E_{\mathrm{H}} &= E_{\mathrm{C_3H_8}} - E^{\Xi}_{\mathrm{C_3H_7O^*OH^*}}\\ &\approx E_{\mathrm{C-H}} - E^{\Xi}_{\mathrm{C-H}} - E^{\Xi}_{\mathrm{O-H}} - E^{\Xi}_{\mathrm{C-O}}. \qquad [\mathrm{A19}]\end{aligned}$$

Similarly,

$$\begin{aligned}\Delta E_{\mathrm{D}} &= E_{\mathrm{C_3D_8}} - E^{\Xi}_{\mathrm{C_3D_7O^*OD^*}}\\ &\approx E_{\mathrm{C-D}} - E^{\Xi}_{\mathrm{C-D}} - E^{\Xi}_{\mathrm{O-D}} - E^{\Xi}_{\mathrm{C-O}}. \qquad [\mathrm{A20}]\end{aligned}$$

Therefore,

$$\begin{aligned}\Delta(\Delta E) &= \Delta E_{\mathrm{H}} - \Delta E_{\mathrm{D}}\\ &= \left(E_{\mathrm{C-H}} - E^{\Xi}_{\mathrm{C-H}} - E^{\Xi}_{\mathrm{O-H}}\right) - \left(E_{\mathrm{C-D}} - E^{\Xi}_{\mathrm{C-D}} - E^{\Xi}_{\mathrm{O-D}}\right)\\ &\approx 0.3\left(E_{\mathrm{C-H}} - E^{\Xi}_{\mathrm{C-H}} - E^{\Xi}_{\mathrm{O-H}}\right). \qquad [\mathrm{A21}]\end{aligned}$$

Combining Eqs. [A18] and [A21], therefore,

$$\mathrm{KIE} = 2.23\, \mathrm{e}^{0.3\left(E_{\mathrm{C-H}} - E^{\Xi}_{\mathrm{C-H}} - E^{\Xi}_{\mathrm{O-H}}\right)/RT}. \qquad [\mathrm{A22}]$$

$0.3E_{\mathrm{C-H}}$ (=4.83 kJ) can be obtained from the literature (19). At 593 K, the maximum KIE will be 6 when no lattice oxygen participates in the C–H bond activation. However, when lattice oxygens are involved (i.e., formation of C–O and O–H bonds as well as the weakening of the C–H bond), the KIE value becomes smaller than 6.

ACKNOWLEDGMENTS

This work was supported by the Director, Office of Basic Energy Sciences, Chemical Sciences Division of the U.S. Department of Energy under Contract DE-AC03-76SF00098. The authors acknowledge Mr. Yihan Shao for calculating the moment of inertia of molecular propane.

REFERENCES

1. Blasko, T., and López Nieto, J. M., *Appl. Catal. A* **157**, 117 (1997).
2. Kung, H. H., *Adv. Catal.* **40**, 1 (1994).
3. Albonetti, S., Cavani, F., and Trifiro, F., *Catal. Rev.-Sci. Eng.* **38**, 413 (1996).
4. Centi, G., and Triffiro, F., *Appl. Catal. A* **143**, 3 (1996).
5. Mamedov, E. A., and Cortés—Corberan, V., *Appl. Catal. A* **127**, 1 (1995).
6. Andersson, S. L. T., *Appl. Catal. A* **112**, 209 (1994).
7. Creaser, D., and Andersson, B., *Appl. Catal. A* **141**, 131 (1996).
8. Chen, K., Khodakov, A., Yang, J., Bell, A. T., and Iglesia, E., *J. Catal.* **186**, 325 (1999).
9. Khodakov, A., Yang, J., Su, S., Iglesia, E., and Bell, A. T., *J. Catal.* **177**, 343 (1998).
10. Khodakov, A., Olthof, B., Bell, A. T., and Iglesia, E., *J. Catal.* **181**, 205 (1999).
11. Iglesia, E., Baumgartner, J. E., and Price, G. L., *J. Catal.* **134**, 549 (1992).
12. Price, G. L., and Iglesia, E., *Ind. Eng. Chem. Res.* **28**, 839 (1989).
13. "CRC Handbook of Chemistry and Physics," 71st ed., pp. 9–95. CRC Press, Boca Raton, FL, 1990.
14. Pepera, M. A., Callahan, J. L., Desmond, M. J., Milberger, E. C., Blum, P. R., and Bremer, N. J., *J. Am. Chem. Soc.* **107**, 4883 (1985).
15. Adams, C. R., and Jennings, T. J., *J. Catal.* **2**, 63 (1963).
16. Adams, C. R., and Jennings, T. J., *J. Catal.* **3**, 549 (1964).
17. Kranzke, L. D., and Keulks, G. W., *J. Catal.* **64**, 295 (1980).
18. Boudart, M., and Djéga-Mariadassou, "Kinetics of Heterogeneous Catalytic Reactions." Princeton Univ. Press, Princeton, NJ, 1984.
19. Ozaki, A., "Isotopic Studies of Heterogeneous Catalysis," Kodansha, Tokyo, 1977.